5340 *Chem. Mater.* **2010,** *22,* 5340–5344
DOI:10.1021/cm101746z

CHEMISTRY OF MATERIALS
Article

Synthesis of Highly Magnetic Iron Carbide Nanoparticles via a Biopolymer Route

Zoë Schnepp,[†] Stuart C. Wimbush,[‡] Markus Antonietti,[†] and Cristina Giordano*[,†]

[†]*Max Planck Institute of Colloids and Interfaces, Research Campus Golm, D-14424 Potsdam, Germany, and* [‡]*Department of Materials Science and Metallurgy, University of Cambridge, Cambridge CB2 3QZ, U.K.*

Received June 22, 2010. Revised Manuscript Received August 4, 2010

In this article, we report a facile, one-pot route to phase-pure Fe_3C nanoparticles (mean diameter = 20 nm) that show a remarkably high saturation magnetization (~130 emu/g), higher than iron oxide (Fe_3O_4) and comparable to that of bulk Fe_3C (~140 emu/g). A readily available biopolymer (gelatin) is used as a matrix to disperse an aqueous iron acetate precursor. On heating, the biopolymer induces nucleation of magnetite (Fe_3O_4) nanoparticles before decomposing to form a carbon-rich matrix. This then acts as a reactive template for carbothermal reduction of the magnetite nanoparticles to Fe_3C at a moderate temperature of 650 °C. This method represents a considerable advance over previous reports that often use high-energy procedures or costly and hazardous precursors. These homogeneous, highly magnetic nanoparticles have many potential applications in biomedicine and catalysis.

Introduction

Magnetic nanoparticles have numerous applications, particularly as recoverable catalysts[1] and in the biomedical sciences.[2] For example, functionalized nanoparticles have been employed in site-specific drug delivery,[3] hyperthermia treatment,[4] and as contrast agents in magnetic resonance imaging (MRI).[5] By far the most widely used and studied material is iron oxide, in the form of magnetite (Fe_3O_4) and maghemite (γ-Fe_2O_3). However, iron oxide nanoparticles demonstrate relatively low magnetic saturation, a crucial factor for many applications. Metallic iron has a much higher saturation magnetization but is unsuitable for medical applications due to its toxicity. An attractive alternative, offering both high magnetic saturation and chemical stability, is iron carbide (Fe_3C).

As with many metal carbide materials, the synthesis of Fe_3C nanoparticles presents a considerable challenge. Many of the well established routes to metal or metal oxide nanoparticles, such as microemulsion or coprecipitation syntheses, are unsuitable for metal carbide formation. The synthesis of phase-pure Fe_3C is particularly difficult since the relatively high-temperature and reducing conditions characteristic of many carbide syntheses often result in the formation of metallic iron or mixed Fe/Fe_3C[6,7] products. While some routes, such as flame spray pyrolysis,[8] have been used to synthesize phase-pure Fe_3C, most current methods involve multiple-step or high-energy procedures using hazardous or costly chemical precursors.[9−11]

A recent advance in the synthesis of carbide materials has been the use of organic gelators. Small molecules such as urea[12,13] or polymers such as chitosan[14] have been employed to disperse soluble metal precursors within a homogeneous gel network. On heating in an inert atmosphere, the gel then decomposes and acts as a carbon source for carbide formation. Biopolymers are particularly useful for this method due to their diverse functionality, which means that they can be used to strongly bind and disperse metal precursors. Furthermore, many biopolymers display remarkable thermal stability; for example, chitosan is resistant to decomposition up to 327 °C in nitrogen.[15] Crucially, in the typically high-temperature synthesis of metal carbides, this means that the polymeric

*Corresponding author. E-mail: Cristina.Giordano@mpikg.mpg.de.

(1) Yi, D. K.; Lee, S. S.; Ying, J. Y. *Chem. Mater.* **2006**, *18*, 2460.
(2) Lu, A.-H.; Salabas, E. L.; Schuth, F. *Angew. Chem., Int. Ed.* **2007**, *46*, 1222.
(3) Lee, J. E.; Lee, N.; Kim, H.; Kim, J.; Choi, S. H.; Kim, J. H.; Kim, T.; Song, I. C.; Park, S. H.; Moon, W. K.; Hyeon, T. *J. Am. Chem. Soc.* **2010**, *132*, 552.
(4) Mornet, S.; Vasseur, S.; Grasset, F.; Duguet, E. *J. Mater. Chem.* **2004**, *14*, 2161.
(5) Lee, J. H.; Huh, Y. M.; Jun, Y. W.; Seo, J. W.; Jang, J. T.; Song, H. T.; Kim, S.; Cho, E. J.; Yoon, H. G.; Suh, J. S.; Cheon, J. *Nat. Med.* **2007**, *13*, 95.
(6) Wang, J. N.; Zhang, L.; Yu, F.; Sheng, Z. M. *J. Phys. Chem. B.* **2007**, *111*, 2119.
(7) Nikitenko, S. I.; Koltypin, Y.; Felner, I.; Yeshurun, I.; Shames, A. I.; Jiang, J. Z.; Markovich, V.; Gorodetsky, G.; Gedanken, A. *J. Phys. Chem. B.* **2004**, *108*, 7620.
(8) Herrmann, I. K.; Grass, R. N.; Mazunin, D.; Stark, W. J. *Chem. Mater.* **2009**, *21*, 3275.
(9) Huo, J.; Song, H.; Chen, X.; Lian, W. *Carbon* **2006**, *44*, 2849.
(10) Sajitha, E. P.; Prasad, V.; Subramanyan, S. V.; Kumar Mishra, A.; Sarkar, S.; Bansal, C. *J. Phys.: Condens. Matter* **2007**, *19*, 046214.
(11) Lee, D. W.; Yu, J. H.; Kim, B. K.; Jang, T. S. *J. Alloys Compd.* **2008**, *449*, 60.
(12) Giordano, C.; Erpen, C.; Yao, W. T.; Milke, B.; Antonietti, M. *Chem. Mater.* **2009**, *21*, 5136.
(13) Giordano, C.; Erpen, C.; Yao, W. T.; Antonietti, M. *Nano Lett.* **2008**, *8*, 4659.
(14) Holgate, M. W. R.; Schoberl, T.; Hall, S. R. *J. Sol-Gel Sci. Technol.* **2009**, *49*, 145.
(15) Hong, P.-Z.; Li, S.-D.; Ou, C.-Y.; Li, C.-P.; Yang, L.; Zhang, C.-H. *J. Appl. Polym. Sci.* **2007**, *105*, 547.

Published on Web 08/24/2010

template is retained for a large proportion of the calcination step. As a result, the complex tertiary structure of the biopolymer may be able to control the nucleation and growth of crystalline intermediates and thus influence the size and morphology of the product. Similar methods are now well established in the synthesis of metal oxide nanostructures.[16]

In this article, we demonstrate the use of gelatin, a readily available biopolymer, for the synthesis of phase-pure Fe_3C nanoparticles. Gelatin is a polypeptide that is manufactured by acid or base hydrolysis of collagen and it forms strong gels in water. By dispersing an aqueous iron precursor within this gel, we show how the polymer controls the nucleation of magnetite nanoparticles within the gel matrix. Using thermogravimetric analysis, mass spectrometry, and elemental analysis (TGA, MS, and EA), we then show that the biopolymer decomposes to form a carbon- and nitrogen-rich matrix around the intermediary oxide nanoparticles. This reactive template then induces carbothermal reduction of iron oxide to iron carbide. In this way, we show how the biopolymer stability, functional groups, and elemental composition all balance to create a stable, phase pure, and structurally uniform product. Finally, we demonstrate the general applicability of this method, using two polysaccharide-based biopolymers (chitosan and alginate) to produce iron carbide nanoparticles (10−30 nm). The highly magnetic nanoparticles described in this article have numerous potential applications in biomedicine and catalysis. In addition, this simple aqueous route represents a considerable advance on previous methods and could be readily applied to a general synthesis of metal carbide materials.

Experimental Section

Gelatin (2 g, Type A from porcine skin, Sigma #G2500) was dissolved in deionized water (100 mL) at 90 °C to form a clear, colorless solution. On cooling, this solution formed a gel that can be converted back to a liquid by heating to approximately 60 °C. An ammonium alginate solution (2%) was prepared by stirring alginic acid (2 g, FMC Biopolymer) in deionized water (100 g). Ammonium hydroxide was added dropwise to dissolve the solid and give a final pH of 6.5. A chitosan solution was prepared by stirring chitosan flakes (2 g, 75−85% deacetylated, Aldrich #448869) in aqueous acetic acid (100 g, 2%) for 24 h. The iron precursor solution was prepared by dissolving iron(II)acetate (1 g, Aldrich, 95%) in deionized water (10 mL) to give a dark brown solution. To synthesize iron carbide, the iron acetate solution (6 g) was added dropwise to the biopolymer solution (5 g) with fast stirring. Gelatin and chitosan formed clear, brown, viscous solutions, while alginate cross-linked to form a thick gel. These products were cast to Petri dishes and dried at 50 °C in air to give clear red/brown films (gelatin and chitosan) or mottled red/brown films (alginate). The resulting films were calcined at 2 °C/min to 650 °C in lidded crucibles in a box furnace under a flow of nitrogen and cooled immediately. It is important to note that for good reproducibility the oxidized form of iron acetate should be used. Iron(II)acetate is oxidized in air to iron(III)acetate or basic iron acetate, with a dark red/brown color. It was this oxidized form that was used for these experiments since the ferrous salt has considerably lower solubility and resulted in precipitation of iron acetate out of the biopolymer on drying. For fresher samples of iron(II)acetate, it was found that the addition of a few drops of H_2O_2 to the dispersion in water could effect the same oxidation to the highly soluble ferric salt. Details of characterization techniques are included in Supporting Information.

Results and Discussion

Calcination of a thin, brown film of iron acetate in gelatin resulted in a shiny, silvery-black solid with the film shape retained. A powder X-ray diffraction (PXRD) pattern of the sample showed peaks characteristic of orthorhombic Fe_3C (*Pnma*, ICCD 00-035-0772) with no crystalline impurity phases (Figure 1a). The sample was stable in air at room temperature, and minimal oxidation occurred on sustained heating at 100 °C. TGA of the sample in air suggested that the onset of oxidation (detected by an increase in the sample mass) occurred at 150 °C. No oxidation was observed when the sample was shaken overnight in water, NaOH (0.1 M), or HCl (0.1M). Elemental analysis detected levels of carbon and nitrogen of 25% and 2%, respectively, suggesting that some amorphous carbon was left in the sample as a side product. Considering that pure Fe_3C should contain 6.7% carbon by mass, the actual content of pure Fe_3C can be estimated as 78%. Scanning electron microscopy (SEM) images (Figure 1b) showed the structure of the calcined film to be composed of a homogeneous network of nanoparticles. This nanoparticulate structure was confirmed using transmission electron microscopy (TEM) (Figure 1c) and the mean particle diameter calculated to be 20 nm (σ = 10%). Figure 1d shows the magnetic hysteresis loop of the powdered sample recorded on a superconducting quantum interference device (SQUID) at 298 K. The magnetization curve is characteristic of a ferromagnetic material and reaches a saturation magnetization of 104 emu/g at 50 kOe. The coercivity and remanence (470 Oe and 20 emu/g respectively) are typical of Fe_3C nanoparticles, as the size of the particles approaches the size of a single magnetic domain. Using the Fe_3C yield calculated above, the saturation magnetization of the Fe_3C content of the sample was found to be 133 emu/g, close to the literature value of 140 emu/g.[17]

In order to investigate the mechanism of formation of the iron carbide from gelatin, samples were quenched at various points during calcination. PXRD patterns of these samples (Figure 2) show that the first crystalline phase was magnetite (Fe_3O_4, ICCD 00-019-0629), which was formed between 300 and 400 °C. Magnetite then persisted as a primary phase up to 600 °C, with partial reduction to wustite (FeO, ICCD 00-006-0615) between 500 and 600 °C. The subsequent transformation from iron oxide to the iron carbide product occurred remarkably quickly, with complete disappearance of the crystalline oxide peaks between 600 and 650 °C. This transformation was associated with an intermediate crystalline

(16) Schnepp, Z.; Wimbush, S. C.; Mann, S.; Hall, S. R. *Adv. Mater.* **2008**, *20*, 1782.

(17) Hofer, L. J. E.; Cohn, E. M. *J. Am. Chem. Soc.* **1959**, *81*, 1576.

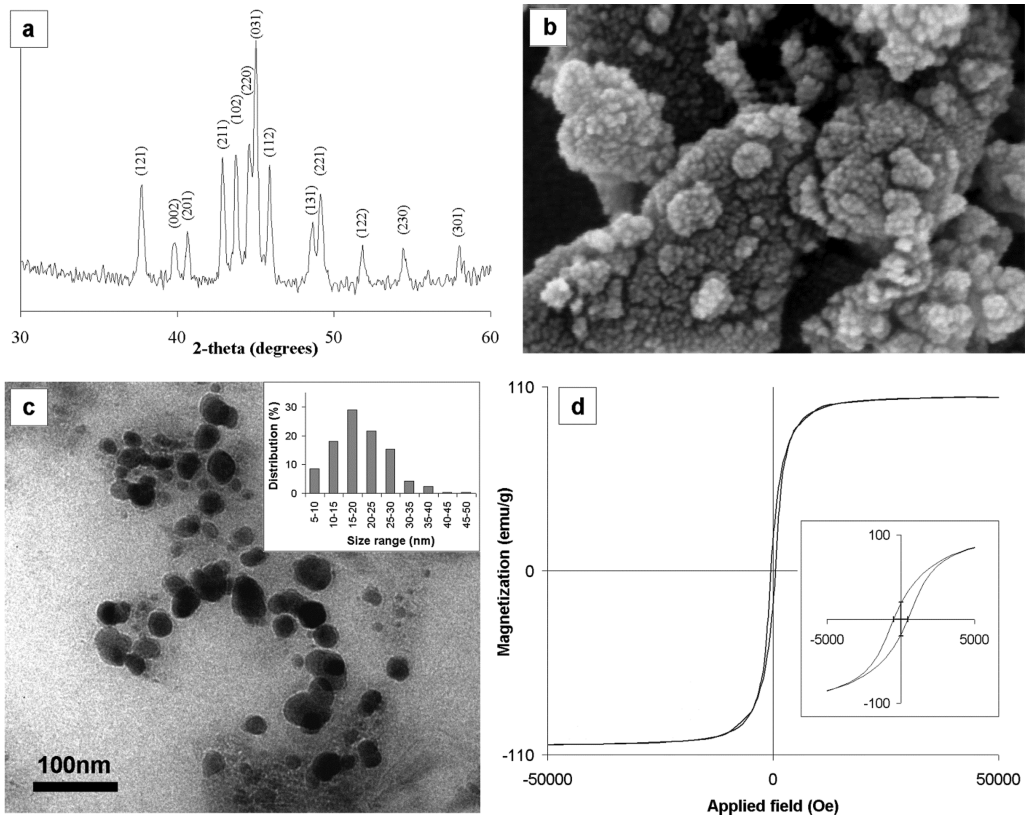

Figure 1. (a) PXRD pattern, (b) SEM image, (c) TEM image, and (d) SQUID magnetometry profile of iron carbide nanoparticles synthesized from gelatin.

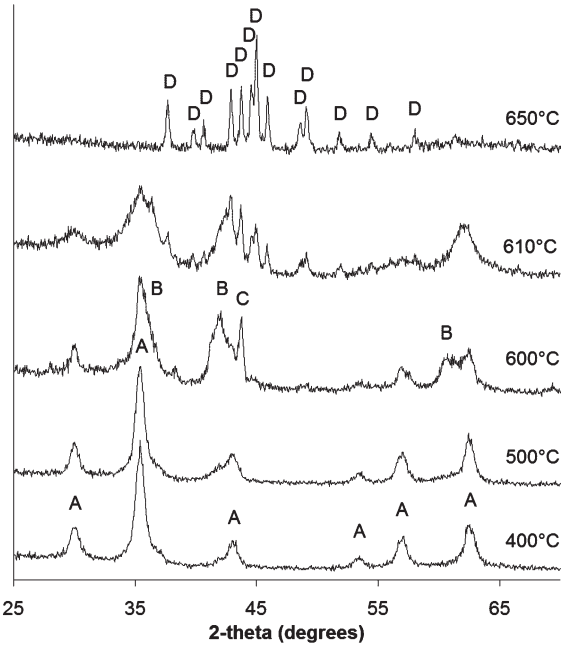

Figure 2. PXRD patterns for samples quenched at various temperatures during the synthesis of Fe_3C from gelatin showing peaks for (A) Fe_3O_4, (B) FeO, (C) $Fe_{1.9}C_{0.1}$, and (D) Fe_3C.

carbon-doped iron phase ($C_{0.1}Fe_{1.9}$ ICDD 00-044-1292). The broad peaks observed in the XRD patterns suggested that this phase was present as nanoparticles, which was confirmed with TEM images and corresponding selected area electron diffraction (Figure S1, Supporting Information) of a sample quenched at 500 °C. These images suggested that the iron oxide nanoparticles, visible as dark spots, were embedded in an amorphous matrix. Elemental analysis of this sample showed over half of the mass to be composed of carbon (27%) and nitrogen (28%), suggesting that the amorphous matrix was formed from decomposition products of the gelatin starting material.

Further insight into the mechanism of iron oxide and iron carbide formation was found using TGA coupled with mass spectrometry (TGA-MS). A summary of these data, together with the key observations from XRD and EA, are shown in Figure 3. Full MS data for all of the ionic species, plotted against the mass loss of the sample when heated in an inert atmosphere are included in Supporting Information (Figure S2). The initial mass loss from 20 to 200 °C is due to the vaporization of free and bound water, possibly coupled with the loss of acetic acid released during the binding of iron to carboxylate groups of the gelatin. The steeper section of the mass loss curve, between 190 and 350 °C, is concurrent with previous reports for the decomposition of gelatin in an inert atmosphere. Mass spectrometry coupled with the TGA during this decomposition region showed peaks for CO_2 (293 °C), HCN (280 °C), H_2O (205 °C, 235 °C), and NH_3 (290 °C), consistent with partial decomposition of the gelatin. Porcine gelatin is composed of multiple amino acids; therefore, it is not possible to define an exact source for each of these emission products. In addition, the decomposition of iron acetate (190−200 °C) also accounts for part of this mass loss. Crucially, this major decomposition step occurs during the same temperature range as that of the nucleation of

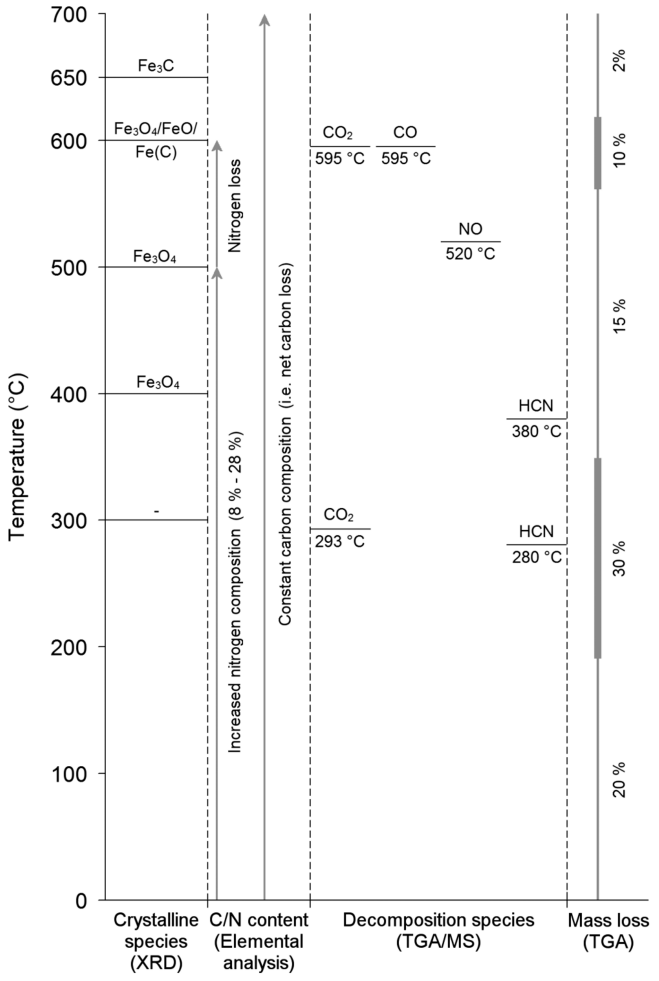

Figure 3. Summary of the key crystalline phases, elemental composition, mass loss, and evolved species during the synthesis of Fe_3C from gelatin.

magnetite nanoparticles. In this way, the dispersed oxide nanoparticles and the carbon- and nitrogen-rich amorphous matrix are formed simultaneously.

Elemental analysis of the samples quenched at 100 °C intervals suggested that the main loss of nitrogen from the reaction mixture occurred between 500 and 600 °C (Figure S3, Supporting Information). This is consistent with the observation of a nitrogen oxide emission at 520 °C from the TGA-MS data and also the partial reduction of Fe_3O_4 to FeO observed from XRD patterns. These data suggest that the nitrogen content of the amorphous matrix is lost through the reaction with the magnetite nanoparticles, leaving the iron oxide nanoparticles embedded in an amorphous carbon-rich matrix. The final crystallographic transformations to form the Fe_3C product coincide with a sharp mass loss of 10% between 575 and 620 °C. Corresponding mass spectrometry indicated emission peaks of CO_2 and CO at 595 °C, suggesting that the iron oxide nanoparticles react with the surrounding carbon-rich matrix to form Fe_3C nanoparticles.

The occurrence of iron oxide nanoparticles as an intermediate phase in this mechanism can be rationalized by considering the microstructure and composition of the biopolymer starting material. Indeed, there are multiple reports of the synthesis of metal oxide nanoparticles using biopolymer templates. Some authors argue that the formation of nanoparticles is merely a factor of spatial separation within the polymer matrix, but most agree that the metal-binding capacity of biopolymers plays a crucial role. Gelatin is composed of a mixture of amino acids, including glycine, proline, hydroxyproline, alanine, glutamic acid, aspartic acid, and arginine,[18] and thus has multiple functionalities that provide sites for metal cation binding. By dispersing the precursor iron cations within a functional aqueous gel, a stabilized homogeneous mixture of the metal precursor is formed (Figure 4). Consequently, the initial nucleation of the iron oxide phase is constrained to nanoparticles. The polymer simultaneously decomposes around these nanoparticles, producing a carbon- and nitrogen-rich template that prevents sintering of the oxide phase. On further heating, we propose that this template reacts with the iron oxide, forming Fe_3C nanoparticles.

To investigate the scope of this mechanism in other functional biopolymers, an identical synthesis procedure was carried out using alginate and chitosan. Alginate is a carboxylate-rich polysaccharide comprising α-L-guluronate (G) and β-D-mannuronate (M) epimers. It is well known for its ability to strongly bind metal cations into cross-linked arrays through a mechanism known as the egg-boxmodel.[19] Chitosan (2-amino-2-deoxy-β(1→4)-D-glucan), sourced from crustacean exoskeletons, is also a polysaccharide but is characterized by amine rather than carboxylate functional groups. The binding of metals to chitosan is understood to occur via ligand interactions with the lone-pair electrons of the amine groups. Calcination of dried gels of alginate and chitosan containing iron acetate resulted in the formation of shiny black solids that were strongly ferromagnetic at room temperature. SEM and TEM images (Figures S4 and S5, Supporting Information) showed nanoparticulate structures for both samples similar to that observed with gelatin, and pXRD showed peaks characteristic of Fe_3C. However, the sample synthesized from chitosan showed an additional peak for metallic iron. XRD profiles of samples quenched at various intervals during calcination also showed a pattern similar to that of the gelatin synthesis (Figure S6, Supporting Information). All syntheses formed magnetite as the initial crystalline phase, followed by partial reduction to FeO and a fast transformation to Fe_3C between 600 and 650 °C. Furthermore, TEM images of samples quenched at 500 °C showed the same structure of Fe_3O_4 nanoparticles embedded in an amorphous matrix (Figure S7, Supporting Information). This suggests that despite the differing composition and structure, the same general mechanism of controlled nucleation and simultaneous polymer decomposition operates in the three biopolymers.

(18) Nguyen, Q.; Fanous, M. A.; Kamm, L. H.; Khalili, A. D.; Schuepp, P. H.; Zarkadas, C. G. *J. Agric. Food Chem.* **1986**, *34*, 565.
(19) Grant, G. T.; Morris, E. R.; Rees, D. A.; Smith, P. J. C.; Thom, D. *FEBS Lett.* **1973**, *32*, 195.

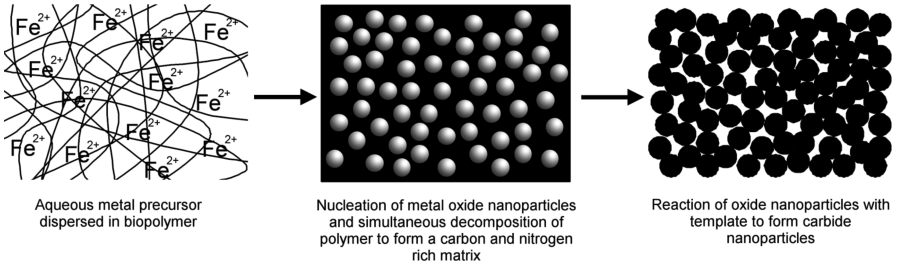

Figure 4. Proposed mechanism for the formation of Fe_3C nanoparticles from a biopolymer gel precursor.

Conclusions

In summary, we have demonstrated a facile and controlled method for the synthesis of highly magnetic iron carbide nanoparticles. Using multiple techniques, we have shown that the reaction proceeds through the nucleation of magnetite nanoparticles with simultaneous decomposition of the polymer. The resulting carbon- and nitrogen-rich matrix prevents sintering of the iron oxide nanoparticles before they finally undergo carbothermal reduction to produce Fe_3C nanoparticles in high yield, with no crystalline byproduct. These highly magnetic nanoparticles should be of great interest for applications in catalysis and biomedicine. To the best of our knowledge, this is the first detailed mechanistic study of the formation of carbide nanoparticles from a gel-precursor. Consequently, this simple and general method should find numerous applications in the largely unexplored synthesis of binary, ternary, and quaternary metal carbides.

Acknowledgment. Z.S., M.A., and C.G. thank the BASF Company and the Max Planck Society for financial support. S.C.W. is supported by The Leverhulme Trust with supplementary funding from The Isaac Newton Trust. We are also grateful to Ms. S. Pirok for elemental analysis, Dr. D. Portehault for TGA-MS measurements, and Dr J. Hartmann for high-resolution SEM imaging.

Supporting Information Available: Images and SAED of intermediate magnetite nanoparticles, full TGA-MS data, elemental analysis tables, images, and XRD profiles for the synthesis of Fe_3C from alginate and chitosan. This material is available free of charge via the Internet at http://pubs.acs.org.